J. Membrane Biol. 142, 195–207 (1994)

The Journal of
Membrane
Biology

Quinine and Quinidine Inhibit and Reveal Heterogeneity of K-Cl Cotransport in Low K Sheep Erythrocytes

N.C. Adragna, P.K. Lauf

Departments of Pharmacology and Toxicology, and Physiology and Biophysics, Wright State University, School of Medicine, Dayton, Ohio 45401-0927

Received: 1 March 1994/Revised: 29 July 1994

Abstract. Low K (LK) sheep red blood cells (SRBCs) serve as a model to study K-Cl cotransport which plays an important role in cellular dehydration in human erythrocytes homozygous for hemoglobin S. Cinchona bark derivatives, such as quinine (Q) and quinidine (QD), are effectively used in the treatment of malaria. In the present study, we investigated in LK SRBCs, the effect of various concentrations of Q and QD on Cl-dependent K efflux and Rb influx (K(Rb)-Cl flux), activated by either swelling in hyposmotic media, thiol alkylation with *N*-ethylmaleimide (NEM), or by cellular Mg (Mg_i) removal through A23187 in the presence of external chelators. K efflux or Rb influx were determined in Cl and NO_3 medium and K(Rb)-Cl flux was defined as the Cl-dependent (Cl minus NO_3) component. K(Rb)-Cl flux stimulated by all three interventions was inhibited by both Q and QD in a dose-dependent manner. Maximum inhibition of K(Rb)-Cl flux occurred at Q and QD concentrations $\geqslant 1$ mM. The inhibitory effect of Q was manifested in Cl, but not in NO_3, whereas QD reduced K and Rb fluxes both in Cl and NO_3 media. The mean 50% inhibitory concentration (IC_{50}) of Q and QD to inhibit K(Rb)-Cl flux varied between 0.23 and 2.24 mM. From determinations of the percentages of inhibition of the different components of K and Rb fluxes, we found that SRBCs possess a Cl-dependent QD-sensitive and a Cl-dependent QD-insensitive K efflux and Rb influx. These two components vary in magnitude depending on the manipulation and directional flux, but in average they are about 50% of the total Cl-dependent flux. This study raises the possibility that, in SRBCs, the Cl-dependent K(Rb) fluxes are heterogeneous.

Correspondence to: N.C. Adragna

Key words: Sheep erythrocytes — K-Cl cotransport — Quinine — Quinidine — Cinchona bark derivatives

Introduction

Cinchona bark derivatives, such as quinine (Q) and quinidine (QD), are extensively used in the treatment of malaria [33, 35, 39]. This subject is attracting attention due to an increased incidence in human malaria during the last two decades caused in part by resistance of the malaria parasite, *Plasmodium* (P.) *falciparum,* to traditional treatment [23, 35, 40]. Although the incidence of malaria attacks is lower in patients homozygous and heterozygous for hemoglobin S (SS and AS, respectively) asymptomatic carriage of the parasite appears to worsen the course of sickle cell disease [15].

An important step in the elucidation of the mechanism of action of Q and QD is to know the mechanism by which these amphiphilic amines penetrate the cells and produce their actions. In the colonic mucosa of rat intestine, the major mechanism of Q transport is by passive diffusion through the cell membrane [29]. In polymorpho-nuclear neutrophils, Q can reach an intracellular/extracellular concentration ratio of more than 100-fold and is found mainly in the soluble fraction of disrupted cells and, in part, reversibly associated with cell structures such as the membrane; thus, Q appears to penetrate these cells by active and passive transport mechanisms [12]. QD also concentrates in several tissues, such as skeletal muscle, kidney, liver and heart [5]. In dog myocardium, the concentrations reached were between 2 to 40 times those found in serum [28]. In human red blood cells, QD equilibrates across the membrane with a red cell:plasma partition ratio of 0.82 and a red cell:buffer partition ratio of 4.16. Uptake from buffer solution was linear up to about 150 μg/ml which is equivalent to 0.46

mM [19]. For sheep red cells the partition coefficient for Q and QD are yet unknown. Q and QD are transported by an organic cation/proton antiporter present in the brush border membrane of human proximal tubule [32]. Due to their basic nature, quinoline-containing drugs, such as Q and QD, accumulate in the acid food vacuoles of the intraerythrocytic-stage of *P. falciparum* [35]. In addition, the transfer process of the monoprotonated and diprotonated species of Q at the oil/water interface are simultaneously controlled by diffusion and re-establishment of the altered equilibrium between Q and protons [41].

The actions of these drugs on cellular function is quite diverse. In vitro Q acts as ion channel blocker and Q and QD have been used for this purpose in tissues of almost every major physiological system of different species [6, 7, 10, 16, 20, 34, 37, 38]. Notably, the proposed mechanism by which QD may alter diastolic depolarization is by interacting with the so-called M-gate in the fast Na channel [5]. Moreover, quaternary amines, such as Q and QD, were found to inhibit delayed rectifier K channels with higher affinity than TEA [18].

These drugs also act on oxidative metabolism [8, 30, 31], are used as tools in molecular biology [17] and as anti-multidrug resistance agents [2], and produce significant effects in lipid peroxidation [36] which may be relevant for sickle cell anemia.

Low K (LK) sheep red blood cells (SRBCs) are used as a model to study K-Cl cotransport (for review, *see* Refs. [11] and [26] and references therein) which plays an important role in cellular dehydration in human erythrocytes homozygous for hemoglobin S [3]. Hence, it was of interest to investigate the effect of cinchona bark derivatives on K-Cl cotransport. The aims of this study were: (i) to assess the mechanism of action of these drugs on the system, (ii) if possible, to use them as tools to further uncover its nature, and (iii) to provide useful information for the development of therapeutic strategies in sickle cell anemia.

Materials and Methods

Chemicals

A23187 (Calbiochem, San Diego, CA); NEM: *N*-ethylmaleimide, EDTA: ethylenediaminetetraacetic acid, DMSO: dimethylsulfoxide, quinine hydro-chloride, and quinidine free base (Sigma, St. Louis, MO). All chemical reagents were analytical grade.

Methods

K Efflux Determination

The K efflux rate constant was determined as detailed elsewhere [24]. Briefly, whole blood from LK sheep was obtained by venipuncture and an aliquot was separated to determine the optical density of 1 ml of packed cells from the hematocrit and optical density of a diluted sample. The remaining blood was spun and the plasma and buffy coat were discarded. Packed cells were washed three times with isotonic NaCl and once with isotonic $NaNO_3$ buffer (PBN) of the following composition (mM): 150 $NaNO_3$, 5 $NaPO_4$ buffer, pH 7.4 (277 mOsM). All washes were done at 4°C. At this point, cells were treated as described below. Afterwards, cells were suspended in prewarmed phosphate-buffered Cl or NO_3 flux media and incubated at 37°C in a water bath. Samples to determine K and hemoglobin concentrations at equilibrium [24] were separated immediately, whereas aliquots of cell suspension were taken as a function of time, spun, and the supernatant was separated to read optical density and K concentration by atomic absorption spectrophotometry. Usually, K efflux rate constants were determined from five time points taken within 1 hr. The computation of K efflux rate constants was as described elsewhere [24].

Rb Influx Determination

Rb influx was determined as detailed elsewhere [25]. Briefly the whole blood was subjected to the same initial steps as described for K efflux, except that flux media contained 20 mM RbCl or $RbNO_3$ replacing equimolar concentrations of NaCl or $NaNO_3$. Furthermore, Rb uptake was immediately stopped by delivering aliquots of cell suspensions into chilled $MgCl_2$ washing solutions, spun, the supernatant was discarded and the cells washed three times with chilled $MgCl_2$. Red cell pellets were lysed in hemolyzing solution, and the Rb concentration was determined by emission spectrophotometry, whereas the volume of cells was determined from the optical densities, as described elsewhere [25].

Swelling Activation

For swelling-activation after the isotonic wash in PBN (*see* composition above), cells were spun and washed twice in hypotonic PBN (225 mOsM). Before the last spin, cells were separated in aliquots, spun, the supernatant was discarded and resuspended in prewarmed hypotonic PBCl (240 mOsM) or PBN (225 mOsM) with or without inhibitors (at the concentrations indicated in the figure legends) or Rb salts. K efflux or Rb influx were determined as described above.

Thiol Activation

For thiol alkylation, a duplicate control sample was removed before NEM treatment. Then, cells were spun, resuspended at a 5% Hct in isotonic PBN with or without 1 mM NEM, and incubated 15 min at 37°C. Afterwards, the protocols for determination of K efflux or Rb influx were followed.

Activation by Lowering Mg_i

As for NEM treatment, reduction of Mg_i was performed once the cells were washed with isotonic PBN and a duplicate control sample was separated before treatment with the ionophore A23187. Cells were resuspended at a 10% Hct in isotonic PBN containing 9 μM A23187 plus 1 mM EDTA and incubated for 15 min at 37°C, spun and washed twice with PBN containing, in addition, 1 mM EDTA. Afterwards, the protocols for determination of K efflux and Rb influx were followed.

Quinine (Q) and Quinidine (QD) Treatment

Q hydrochloride was prepared as a 10 mM stock solution in either PBN at the appropriate osmolality or in DMSO. QD was prepared in 10 mM

stock solution in DMSO. In preliminary experiments for Q treatment, cells were either exposed to the drug during the flux period or after a 30 min incubation with Q prior to the flux. Since no difference was found in Q inhibition, the 30 min incubation period was eliminated. Q and QD increased the percentage of hemolysis as a function of time and concentration. The percentage of hemolysis shown in Fig. 3 for K efflux was calculated as follows:

percent hemolysis = $(OD_s \times V_h) \times 100/(OD_h \times DF)$

where OD_s and OD_h are the optical densities of the supernatant and hemolysate, respectively (*see* K efflux determination above), V_h is the volume of hemolysate and DF its dilution factor.

Cell Water Determinations

To determine the effect of Q and QD on cell water content, cells were incubated in solutions containing 5 mM phosphate buffer, pH 7.5, and NaCl at the concentrations of 119, 130, 141, 154, and 184 mM to give 230, 250, 270, 295 and 350 mOsM, respectively, and in the presence and absence of the drugs. The protocol was as follows: packed cells were washed with isotonic NaCl as described above, resuspended at a Hct of 5% in NaCl solution, divided into aliquots, and spun. The supernatant was discarded and cells were resuspended in either PBCl solutions of different osmolalities to which DMSO was added at the same concentration as in the two other conditions, or PBCl solutions of different osmolalities containing, in addition, 2 mM of either Q or QD dissolved in DMSO. Cells were incubated for 30 min at 37°C, spun, concentrated by centrifugation and transferred into three preweighed 1.5 ml Eppendorf tubes. Cell suspensions were spun and supernatants were removed, weighed to obtain wet weights (WWT) and dried for 48 hr at 80°C. At the end of this period, dry weights (DWT) were obtained for determination of water content by calculation of the Kg cell water/Kg dry cell solids (DCS) as follows: (WWT – DWT)/DWT.

Chloride Determination

Intracellular chloride (Cl_i) was determined as detailed elsewhere [27]. Briefly, dry cell pellets obtained, as described above, were resuspended in 1 ml of 7% perchloric acid, vortexed vigorously and kept overnight to extract ions. Cl_i was determined in 100 μl aliquots in a digital chloridometer (HaakeBuchler Instruments, Saddlebrook, NJ).

Statistics

Results are expressed as the mean ± standard error of the mean (X ± SE). Statistical significance was assessed by two-sample paired or unpaired *t*-test analysis with computer software.

Results

Effect of Q and QD on K Efflux

Swelling Activation

Figure 1 shows the effect of increasing Q concentrations on K loss as a function of time in osmotically swollen LK SRBCs. Q inhibited, in a dose-dependent manner, K loss in Cl (*A*) but not in NO_3 (*B*). At 3 mM, Q inhibited K loss in Cl by 68%.

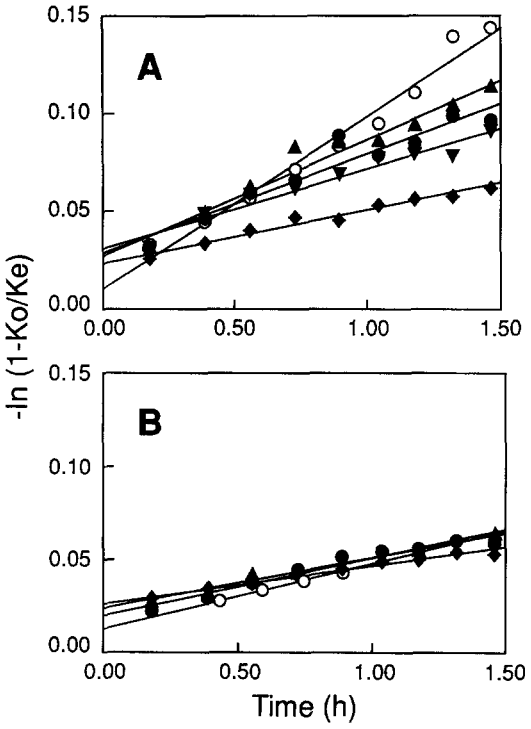

Fig. 1. Q effect on K loss in osmotically swollen LK SRBCs. (*A*) K loss in Cl as a function of time for control (no inhibitor, open circles), 1 (filled triangles), 1.5 (filled circles), 2 (inverted filled triangles), and 3 mM Q (filled diamonds). (*B*) K loss in NO_3 as a function of time with conditions and symbols as in *A*.

Results similar to those observed with Q were obtained upon inhibition of K loss as a function of time with QD. However, in contrast to Q, QD inhibited K loss in NO_3 by about the same percentage as in Cl medium (60 *vs.* 68%, respectively), and the concentration of QD to inhibit by 68% K loss in Cl was 1 mM instead of 3 mM for Q (*results not shown*).

Thiol Activation

The increase in K loss induced by 1 mM NEM treatment was about four- to sixfold in Cl, and four- to sixfold for the Cl-dependent component without activation in NO_3 [26]. Q inhibited K loss in Cl in a dose-dependent manner (*results not shown*).

Figure 2 shows the effect of QD on K loss as a function of time. In contrast to Q, QD inhibited in a dose-dependent manner K loss both in Cl (*A*) and NO_3 (*B* and inset) as described for swelling-activated cells. At 1 mM QD, the inhibition in Cl was about 70% and in NO_3 close to 60%.

Activation by Lowering Mg_i

The effect of Q on K loss as a function of time in A_{23187}-treated (low Mg_i) LK SRBCs was also dose dependent.

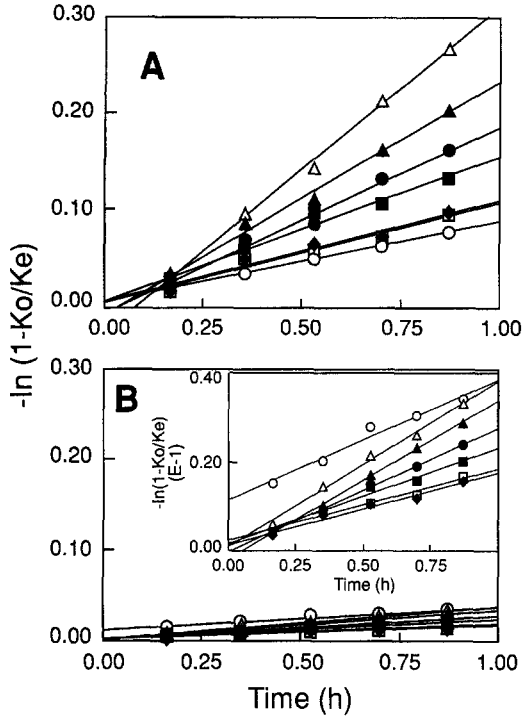

Fig. 2. QD effect on K loss in NEM-treated LK SRBCs. (*A*) K loss in Cl as a function of time for control (open circles), control+ NEM (open triangles) 0.2 (filled triangles), 0.4 (filled circles), 0.6 (filled squares), 0.8 (filled diamonds), or 1.0 mM QD (open squares). (*B*) K loss in NO_3 as a function of time with conditions and symbols as in *A*. (Inset): Same as *B* but in expanded scale.

Treatment with the ionophore stimulated K loss by about twofold in Cl medium. At 2 mM, Q inhibited this component by 87% (*results not shown*).

As in the case of NEM-treated cells, QD inhibited both K loss in Cl and NO_3 medium. At 1.0 mM, the inhibition in Cl was 83% and in NO_3 99% (*results not shown*).

The conclusion from the above experiments is that both Q and QD inhibited K efflux in LK SRBCs in a dose-dependent manner.

Effect of Q and QD on LK SRBC Lysis

Both Q and QD increased cell lysis as a function of time and concentration. Figure 3 shows the percentage of lysis, calculated as described in Materials and Methods, as a function of time of incubation in Cl and NO_3 and in the presence and absence of 3 mM Q. Q increased the percentage of cell lysis by about threefold with respect to the control, both in Cl and NO_3, and the function appeared to be exponential in the presence of the drug but not in the control conditions. Determination of the rate at which lysis occurred was relevant for flux measurements, because this information allowed us to set the flux period to values short enough so that the cells did not reach significant levels of lysis.

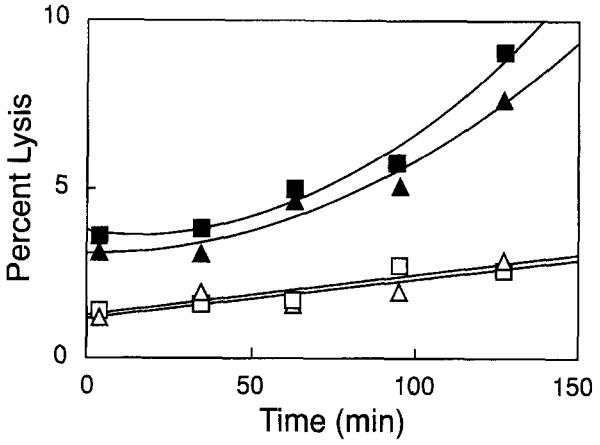

Fig. 3. Effect of Q on cell lysis as a function of time. Control (no Q) in Cl (open squares) and NO_3 (open triangles). Q (3 mM) in Cl (filled squares) and in NO_3 (filled triangles). Percent hemolysis was determined as described in Materials and Methods.

Effect of Q and QD in Cell Volume and Cl Content

Q and QD are organic bases which are freely permeable across the cell membrane and apparently can accumulate in the intracellular compartment [12, 35]. In the event that these drugs were accumulating in SRBCs, we speculated that this could possibly increase the intracellular pH (pH_i) of SRBCs and, thus, inhibit K and Rb fluxes by inducing cell shrinkage. Furthermore, alkalinization should be expected to induce a decrease in cell volume and Cl content and an increase in Cl concentration. To test this hypothesis, cell water and Cl content were determined as described in Materials and Methods as a function of media osmolality.

Figure 4 shows water (*A*) and Cl (*B*) contents, and Cl concentration (C) in cells incubated in the absence and presence of 2 mM Q or QD as a function of the inverse of flux media osmolality. As expected for cellular osmometers, the water content increased in swollen cells and decreased in shrunken cells, and this behavior occurred both in the presence and absence of Q and QD. However, the water content of cells incubated in Q was significantly higher than that of the control ($P < 0.02$, $n = 5$) and that of QD ($P < 0.03$, $n = 5$). QD did not affect the water content with respect to control cells.

The Cl content of LK SRBCs (*B*) was independent of the changes in osmolalities. The mean value of Cl content in control, Q- and QD-treated cells (210 ± 8, 232 ± 11, and 178 ± 5 mEq/Kg DCS, respectively) were significantly different (controls *vs.* Q, $P < 0.003$, control *vs.* QD, $P < 0.00001$, and Q *vs.* QD, $P = 0.0002$, $n = 5$).

The Cl concentration (mEq/Kg cell water) decreased by 18, 17, and 20% in control, Q- and QD-treated cells, respectively, at 230 mOsM, and increased by 14, 12, and 20%, respectively at 350 mOsM. The concentration of Cl was higher for Q ($P = 0.005$, $n = 5$) and lower for QD

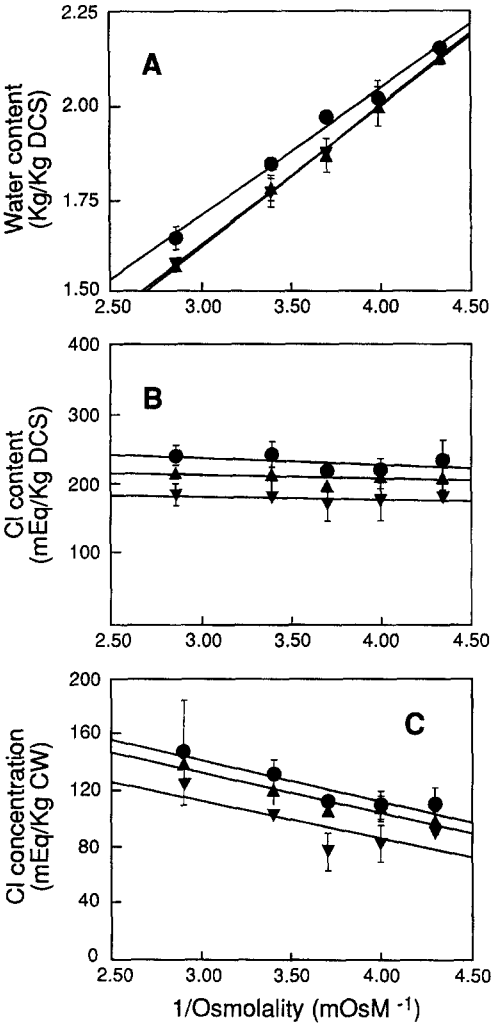

Fig. 4. Effect of Q and QD on water and Cl contents, and Cl concentration as a function of the inverse of medium osmolality (1/Osm) in LK SRBCs. (*A*) Water content before (filled triangles) and after treatment with 2 mM Q (filled circles) and 2 mM QD (inverted filled triangles). Slopes of linear regressions for control, Q and QD *vs.* 1/Osm (± SE, $n = 5$): 368 ± 10, 335 ± 20, and 380 ± 9, respectively. (*B*) Cl content and (*C*) Cl concentration with conditions and symbols as in *A*.

($P = 0.008$, $n = 5$) than for control cells in the entire range of osmolalities tested (*C*).

These findings indicate that the inhibitory action of Q and QD cannot be explained by an alkalinization-induced cell shrinkage caused by drug accumulation in the intracellular compartment. Q actually swelled the cells by about 3% with respect to the control, and swelling is an activator of the system instead of an inhibitor.

Dose-effect Relationships between Q or QD Concentration and K Efflux

Figures 5 and 6 summarize the dose-effect relationship between the concentration of Q and QD, respectively,

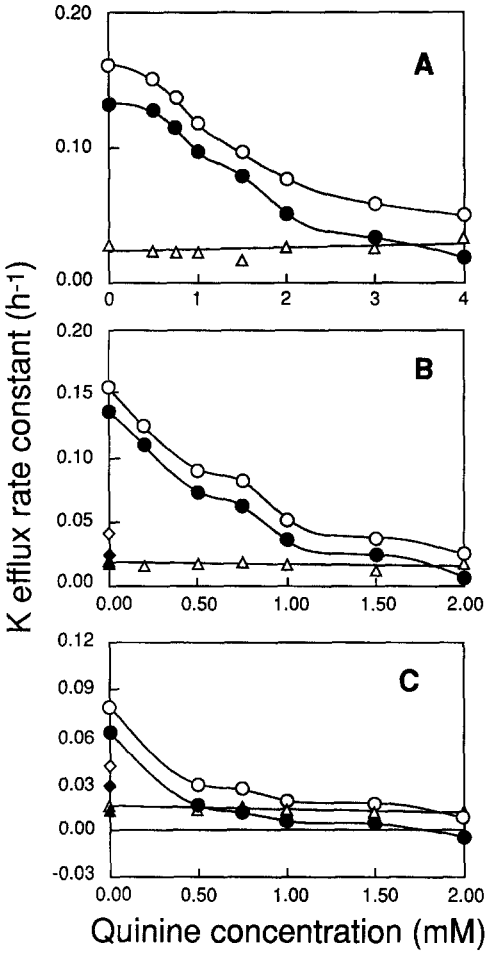

Fig. 5. Dose-effect relationship between the concentration of Q and the rate constants of K efflux in Cl and NO_3 stimulated by three interventions. (*A*) Swelling activation. Open circles, Cl; open triangles, NO_3, and filled circles, Cl-dependent component. (*B*) Thiol alkylation with NEM. Open diamond, Cl control (no NEM); open circles, Cl + NEM; filled triangle, NO_3 control (no NEM); open triangles, NO_3 + NEM; filled diamond, Cl-dependent component control (no NEM); filled circles, NEM-activated Cl-dependent component. (*C*) Cellular Mg removal through A23187 + EDTA. Open diamond, Cl control (no A23187); open circles, Cl + A23187; filled triangle, NO_3 control (no A23187); open triangles, NO_3 + A23187; filled diamond, Cl-dependent component control (no A23187); and filled circles, low Mg_i-activated Cl-dependent component.

and the rate constants of K efflux in Cl an NO_3 and the Cl-dependent component stimulated by three interventions: swelling activation (*A*), thiolalkylation with NEM (*B*), and cellular Mg removal with A23187 + EDTA (*C*).

The figures show that both Q and QD inhibited in a dose-dependent manner K efflux in Cl and the Cl-dependent component as well, and that QD but not Q inhibited K efflux in NO_3. However, Q appeared to induce some inhibition in A23187-treated cells (*compare with* Fig. 3, *B*).

To determine if the mechanism of inhibition of K(Rb)-Cl flux by Q and QD was the same for each

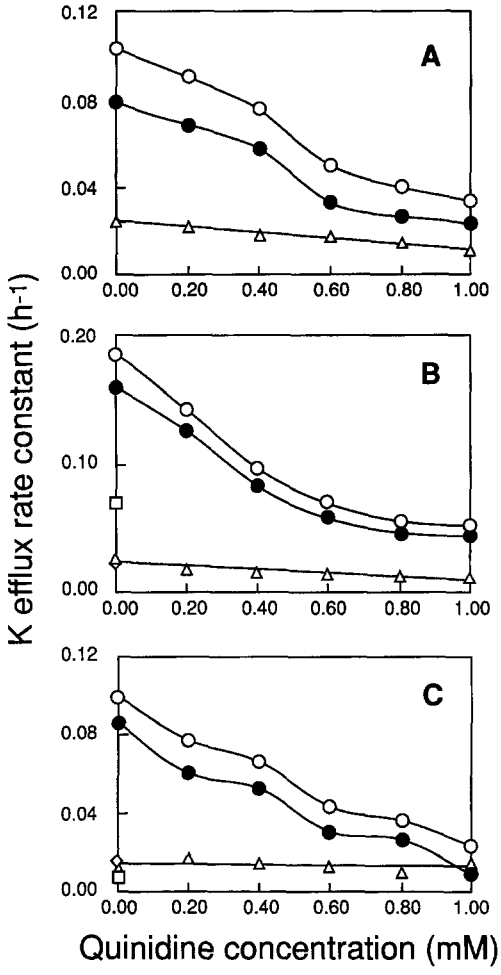

Fig. 6. Dose-effect relationship between the concentration of QD and the rate constants of K efflux in Cl and NO_3 stimulated by three interventions. (*A*) Swelling activation. Open circles, Cl; open triangles, NO_3, and filled circles, Cl-dependent component. (*B*) Thiol alkylation with NEM. Open square, Cl control (no NEM); open circles, Cl + NEM; open diamond, NO_3 control (no NEM); open triangles, NO_3 + NEM; filled circles, NEM-activated Cl-dependent component. (*C*) Cellular Mg removal through A23187 + EDTA. Open diamond, Cl control (no A23187); open circles, Cl + A23187; open square, NO_3 control (no A23187); open triangles, NO_3 + A23187; and filled circles, low Mg_i-activated Cl-dependent component.

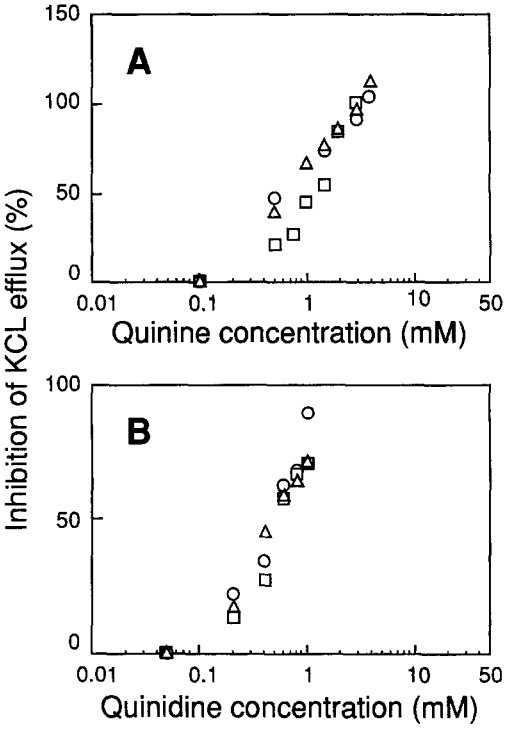

Fig. 7. Inhibition of Cl-dependent K efflux by Q (*A*) and QD (*B*) as a function of drug concentration in logarithmic scale: Open squares, swelling-activated; open triangles, NEM-activated; and open circles, A23187-activated cells. The percentage of inhibition was calculated with respect to the control (without inhibitor) for each manipulation, which was taken as 100%. The curves represent a typical experiment for each condition and drug. IC_{50}s were calculated by regression of the values of Cl-dependent K efflux expressed in percent of the control corresponding to the linear parts of the curves and the drug concentration in arithmetical scale. The equation used was IC_{50} (mM) = (50 − intercept)/slope. *See text* for IC_{50} values.

manipulation and to assess their potency, the percentage of inhibition of the Cl-dependent component activated either by swelling, NEM or A23187 was plotted as a function of the logarithm of Q and QD concentration (Fig. 7, *A* and *B*, respectively). The figure shows in each panel a representative experiment for each mode of activation of K(Rb)-Cl flux. The data indicate that the mechanisms of action of both Q and QD were the same for all three manipulations since the linear portions of the curves were not statistically different. The IC_{50}s to inhibit the Cl-dependent component for this figure were in mM: 1.24, 0.71 and 0.61 for Q and 0.56, 0.48, and 0.48 for QD for swelling, NEM and A23187 activation, respectively (*see* figure legend for determination of IC_{50} values).

To further explore the mechanism of inhibition by the two drugs, Dixon plots were constructed relating the inverse of swelling-activated, Cl-dependent K efflux with the concentration of Q and QD (Fig. 8). The data fitted curvilinear functions, an indication of complex inhibitory kinetics for both Q and QD.

Effect of QD on Rb Influx

In this series of experiments Rb was used as K congener, and the rate of uptake was measured in: (a) hypotonically swollen, (b) NEM-treated, and (c) low Mg_i-activated cells. In efflux experiments we found that the Q-induced lysis was higher than that of QD at all concentrations and time points tested. For this reason and to avoid selecting a population of younger cells which might be more resistant to lysis, we continued the influx studies with QD alone. To minimize lysis (*see* results, Fig. 3), QD was used at 0.1, 0.2, 0.3, 0.5 and 1.0 mM concentrations and

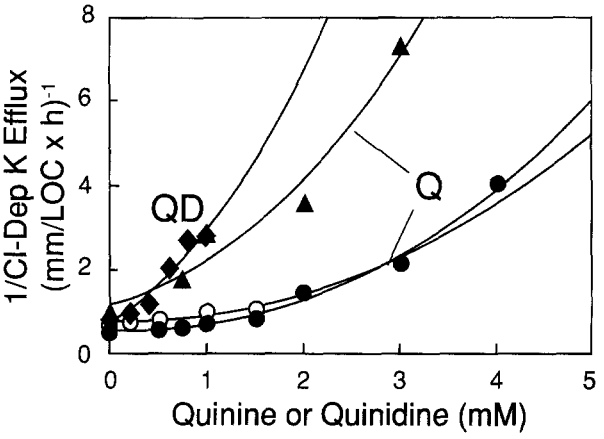

Fig. 8. Dixon plot relating the inverse of swelling-induced Cl-dependent K efflux and Q and QD concentrations. Q open and filled circles and filled triangles. QD, filled diamonds.

the Rb uptake was measured as a function of time in Cl and NO_3. As observed for K efflux, QD inhibited both the uptake in Cl and in NO_3 in a dose-dependent manner (*results not shown*). However, at a concentration of 1 mM, the inhibition of Rb uptake in Cl was about half of that seen for K efflux, whereas in NO_3 the inhibition of the two fluxes was dependent on the manipulation used to activate the cells (*see below* and Table 1).

Dose-Effect Relationship between QD Concentration and Rb Influx

Figure 9 shows the dose-effect relationship between the concentration of QD and Rb influx in Cl and NO_3 and the Cl-dependent component stimulated by three interventions: Swelling activation (*A*), thiolalkylation with NEM (*B*), and cellular Mg removal through A23187+EDTA (*C*).

As for efflux, QD inhibited Rb influx in Cl and NO_3 in a dose-dependent manner, and the Cl-dependent component as well.

To determine if the mechanism of inhibition of RbCl influx by QD was the same for each manipulation and to assess its potency, the percentage of inhibition of the Cl-dependent component activated either by swelling, NEM or A23187 was plotted as a function of the logarithm of QD concentration. These results (*not shown*) indicated that the mechanism of action of QD was the same for all three manipulations since the slope of the curves was not statistically different. The IC_{50}s to inhibit the Cl-dependent Rb influx were in mM: 0.74, 0.66 and 0.92 for swelling, NEM and A23187 activation, respectively.

Inhibition of K and Rb Fluxes by Q and QD

The IC_{50}s of the drug-sensitive components were calculated either as a percentage of the Cl-dependent K(Rb) flux at 0 mM Q or QD [$K(Rb)ClP_o$] or as a percentage of the maximum inhibitable Cl-dependent K(Rb) flux [$K(Rb)ClP_{1(H)}$] (*see below*). The first calculation appeared to us more reliable because it did not require the maximum saturation concentration, whereas the second required this value which due to interexperimental variability was not always observed at 1 mM, especially for Q. Since increasing the drug concentration increased RBC lysis, we arbitrarily took as the maximum inhibitable Cl-dependent K(Rb) flux the value at 1 mM QD for all experiments and the value at the highest concentration available for Q. The following components for K efflux and Rb influx were derived from these calculations and were used in Figs. 10, 11 and 12 and in Tables 2 and 3.

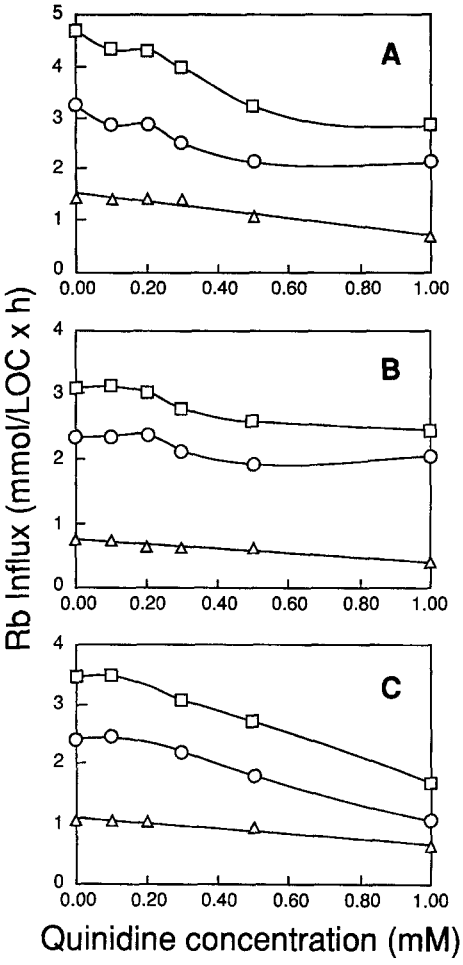

Fig. 9. Dose-effect relationship between the concentration of QD and Cl-dependent Rb influx in Cl and NO_3 stimulated by three interventions. (*A*) Swelling activation. (*B*) Thiol alkylation with NEM. (*C*) Cellular Mg removal through A23187 + EDTA. Open squares for Cl, open triangles for NO_3, and open circles for the Cl-dependent component.

$K(Rb)Cl_o$ = Cl-dependent K(Rb) flux at zero external Q or QD concentration.

$K(Rb)Cl_x$ = Cl-dependent K(Rb) flux at external Q or QD concentration > 0 mM.

$K(Rb)Cl_{1(H)}$ = Cl-dependent K(Rb) flux at external Q or QD = 1 mM (1) or at the highest (H) concentration at which saturation occurred.

$K(Rb)ClP_o$ = Cl-dependent K(Rb)Cl flux sensitive to Q or QD as a fraction of K(Rb)Cl flux at 0 mM drug, in percent = $[K(Rb)Cl_o - K(Rb)Cl_x]/K(Rb)Cl_o$.

$K(Rb)ClP_{1(H)}$ = Cl-dependent K(Rb) flux sensitive to Q or QD as a fraction of K(Rb)Cl flux at 1 mM (1) or at the highest (H) drug concentration, in percent = $[K(Rb)Cl_o - K(Rb)Cl_x]/[K(Rb)Cl_o - K(Rb)Cl_{1(H)}]$.

K(Rb)ClIP = Cl-dependent K(Rb) flux insensitive to Q or QD as a fraction of K(Rb)Cl flux at 0 mM drug, in percent = $K(Rb)Cl_x/K(Rb)Cl_o$.

Figure 10*A*, *B* and *C* shows typical experiments with the three different efflux components, $KClP_o$, $KClP_{1(H)}$ and KClIP, for swelling-, NEM-, and A23187-activated cells, respectively, as a function of Q concentration. In swelling-activated cells, saturation was observed at lower Q concentrations than in NEM- and A23187-activated cells for each of the three parameters. Furthermore, in contrast to panel *A*, $KClP_o$ and $KClP_{1(H)}$ were identical and fully inhibitable by Q in panels *B* and *C*.

Figure 11*A*, *B* and *C* shows typical experiments with the three different efflux components, $KClP_o$, $KClP_{1(H)}$ and KClIP, for swelling-, NEM-, and A23187-activated cells, respectively, as a function of QD concentration. In contrast to Q, the QD-sensitive and -insensitive efflux components behave similarly for the three types of cells, and saturation was observed in most experiments at 1 mM QD.

Figure 12*A*, *B* and *C* shows typical experiments with the three different influx components, $RbClP_o$, $RbClP_{1(H)}$ and RbClIP, for swelling-, NEM-, and A23187-activated cells, respectively, as a function of QD concentration. Interestingly, the general behavior for the three types of cells in influx experiments with QD resembled that of their counterparts in efflux experiments with Q, except that a larger difference between $RbClP_o$ and $RbClP_{1(H)}$ and a larger drug-insensitive component were observed for influx.

The IC_{50}s for Q and QD for the inhibition of KCl and RbCl fluxes are summarized in Table 1. The IC_{50}s estimated from the $[K(Rb)ClP_o]$ and $[K(Rb)ClP_{1(H)}]$ percentages were not different for efflux both for Q and QD, whereas those corresponding to the influxes were statistically different in average ($P = 0.0094$) (*see ALL* for influx in Table 1). In swelling-activated cells, Q appeared to be less potent than for the other two types of cells; however, the IC_{50}s were not statistically different due to the large dispersion of the data.

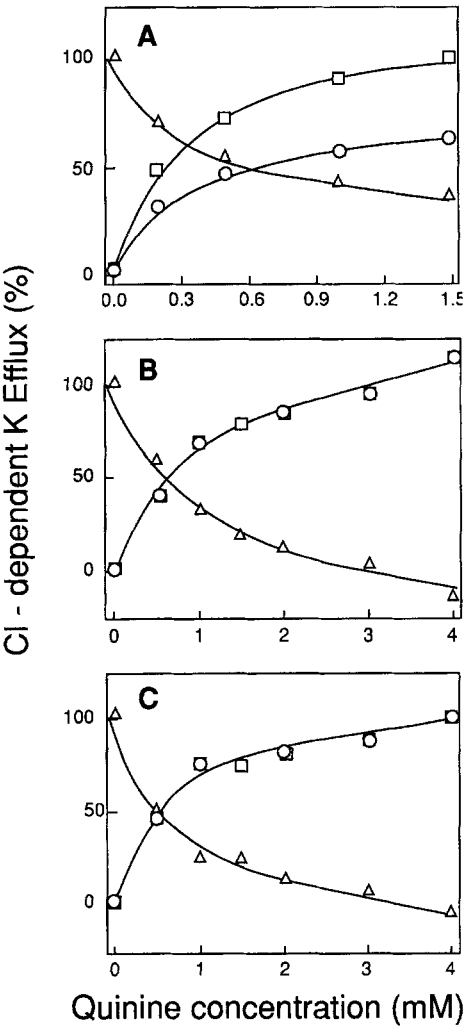

Fig. 10. Dose-effect relationship between the concentration of Q and three derived parameters of K efflux stimulated by three interventions. (*A*) Swelling activation. (*B*) Thiol alkylation with NEM. (*C*) Cellular Mg removal through A23187 + EDTA. Open squares for $KClP_{1(H)}$, open circles for $KClP_o$, and open triangles for KClIP (*see* definitions in Results).

The IC_{50}s determined from the $K(Rb)ClP_{1(H)}$ parameter were statistically similar for both efflux and influx in the three types of cells treated with QD (*see* Efflux/Influx Ratio, Table 1). Furthermore, according to the IC_{50}s determined from $K(Rb)ClP_o$, QD inhibited with the same potency swelling-activated KCl and RbCl flux, and was about twice more potent to inhibit efflux than influx when activated by the other two manipulations.

Table 2 summarizes the percentage of inhibition by 1 mM Q and QD of K efflux and Rb influx in Cl and NO_3 and of the two Cl-dependent and Cl-independent components, as defined above, in cells activated either by hypotonic swelling, NEM treatment or by lowering the

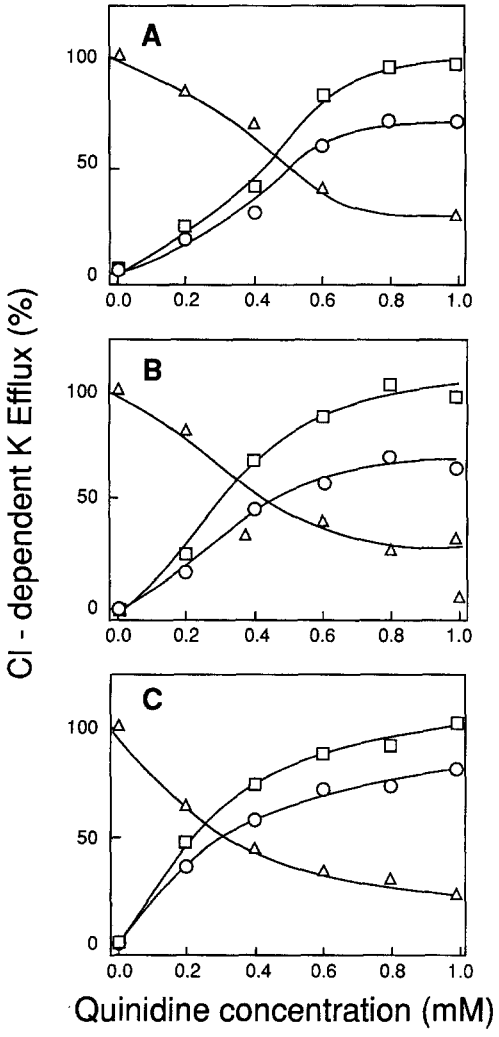

Fig. 11. Dose-effect relationship between the concentration of QD and three derived parameters of K efflux stimulated by three interventions. (*A*) Swelling activation. (*B*) Thiol alkylation with NEM. (*C*) Cellular Mg removal through A23187 + EDTA. Open squares for $KClP_{i(H)}$, open circles for $KClP_o$, and open triangles for KClIP (*see* definitions in Results).

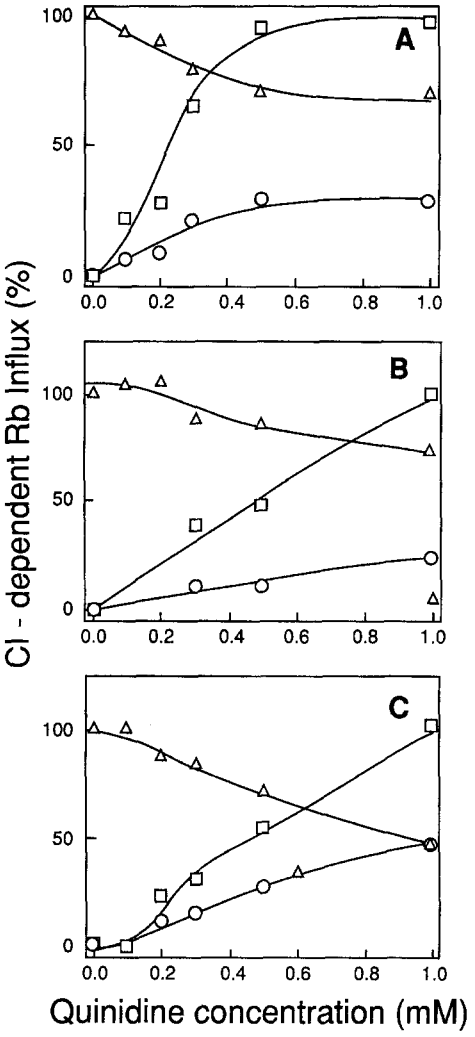

Fig. 12. Dose-effect relationship between the concentration of QD and three derived parameters of Rb influx stimulated by three interventions. (*A*) Swelling activation. (*B*) Thiol alkylation with NEM. (*C*) Cellular Mg removal through A23187 + EDTA. Open squares for $RbClP_{i(H)}$, open circles for $RbClP_o$, and open triangles for RbClIP (*see* definitions in Results).

Mg_i concentrations. The inhibitory action of QD on K efflux was higher than that of Q in NO_3 medium for the three types of cells. Q inhibition of K efflux in NO_3 was not different from zero in swollen cells, but a small inhibition was observed in cells subjected to the other two manipulations.

Comparison of efflux and influx inhibition by QD indicates that, in general, QD was more effective inhibiting efflux than influx with the exception of the $K(Rb)ClP_{i(H)}$ component which was the same in the three types of cells. In swollen cells, the percentage of inhibition of Cl-dependent K efflux at 1 mM drug concentration was about or more than 70% higher for $K(Rb)ClP_{i(H)}$ than for $K(Rb)Cl_o$ for both Q and QD. In contrast, no difference between these components was found for NEM- and A23187-activated cells inhibited by Q. Furthermore, QD inhibition, when expressed as $K(Rb)ClP_{i(H)}$, was 45 and 22% higher for efflux and more than 100% for influx in NEM- and A23187-treated cells, respectively, than when expressed as $K(Rb)ClP_o$.

The Cl-dependent QD-insensitive component was not different for efflux and influx in swollen cells and was about twice higher for influx than efflux in the other two types of cells.

These data indicate that, at least for QD, the inhibition of K(Rb)-Cl flux was asymmetric, with more inhibition of the efflux than of the influx, and more so in thiol-alkylated and low Mg_i cells. This asymmetry could be explained by the existence of a QD-insensitive component larger for influx than efflux. Our findings also

Table 1. Median inhibitory dose (IC_{50}) for quinine (Q) and quinidine (QD) to inhibit Cl-dependent K and Rb fluxes

Drug	Manipulation	IC_{50}					
		Efflux		Influx		Efflux/influx ratio	
		A	B	A	B	A	B
Q	Swelling	1.28 ± 0.23 (8)	0.93 ± 0.20 (8)				
	NEM	0.56 ± 0.08 (3)	0.69 ± 0.11 (3)				
	A23187	0.47 (2)	0.47 (2)				
	ALL	0.99 ± 0.18 (13)[a]	0.81 ± 0.13 (13)[b]				
QD	Swelling	0.69 (2)	0.46 (2)	0.79 (2)	0.41 (2)	0.87	1.12
	NEM	0.40 (2)	0.28 (2)	0.54 ± 0.16 (4)	0.32 ± 0.03 (4)	0.74	0.88
	A23187	0.38 (2)	0.39 (2)	0.84 ± 0.06 (3)[e]	0.45 ± 0.06 (3)[f]	0.45	0.87
	ALL	0.49 ± 0.08 (6)[c]	0.38 ± 0.04 (6)[d]	0.70 ± 0.08 (9)[g]	0.38 ± 0.04 (9)[h]	0.70	1.00

The number of experiments is indicated in parentheses. IC_{50}s were determined from the drug-sensitive components calculated either as a percentage of the total Cl-dependent K(Rb) flux [$K(Rb)ClP_o$ represented as A] or as a percentage of the maximum inhibitable Cl-dependent K(Rb) flux [$K(Rb)ClP_{1(H)}$, represented as B]. (a *vs.* c) $P = 0.0206$; (b *vs.* d) $P = 0.0081$; (e *vs.* f) $P = 0.018$; (g *vs.* h) $P = 0.0094$.

Table 2. Percentage of inhibition of K and Rb fluxes by 1 mM quinine (Q) and quinidine (QD)

Activation	Flux component	Efflux*		Influx*	Efflux/influx ratio
		Q	QD	QD	
Swelling	Cl	33 ± 4 (7)	50 ± 13 (3)	38 (2)	1.3
	NO_3	−3 ± 15 (7)	53 ± 7 (3)	53 (2)	1.0
	$K(Rb)ClP_o$	42 ± 6 (7)	49 ± 15 (3)	32 (2)	1.5
	$K(Rb)ClP_{1(H)}$	69 ± 12 (7)	81 ± 19 (3)	67 (2)	1.2
	K(Rb)ClIP	57 ± 16 (7)	51 ± 15 (3)	69 (2)	0.7
NEM	Cl	63 ± 4 (3)	71 (2)	40 ± 13 (5)	1.8
	NO_3	36 ± 13 (3)	76 (2)	40 ± 13 (5)	1.9
	$K(Rb)ClP_o$	66 ± 6 (3)	69 (2)	40 ± 17 (5)	1.7
	$K(Rb)ClP_{1(H)}$	68 ± 6 (3)	100 (2)	100 ± 0 (5)	1.0
	K(Rb)ClIP	34 ± 6 (3)	31 (2)	60 ± 17 (5)	0.5
A23187	Cl	72 (2)	81 (2)	46 ± 12 (3)	1.8
	NO_3	20 (2)	83 (3)	30 ± 13 (3)	2.8
	$K(Rb)ClP_o$	82 (2)	82 (2)	45 ± 7 (3)	1.8
	$K(Rb)ClP_{1(H)}$	84 (2)	100 (2)	100 ± 0 (3)	1.0
	K(Rb)ClIP	16 (2)	19 (2)	49 ± 13 (3)	0.4

* *See* definitions of components in Results (Tables 2 and 3). Results are expressed in percent.

show a different behavior of swollen cells compared to thiol-alkylated or low Mg_i cells.

Because the absolute values of Cl-dependent Rb influx were higher than those corresponding to K efflux, expression of inhibition in percentage could misleadingly indicate more inhibition of efflux than influx. To account for this difference, we calculated Q- and QD-sensitive Cl-dependent K/Rb fluxes by subtracting from the Cl-dependent flux in the absence of drug (control condition) the corresponding value at 1 mM drug. Table 3 shows that, based on the absolute change of the Cl-dependent efflux and influx induced by 1 mM Q and QD, the KCl efflux/RbCl influx ratio in swelling- and A23187-activated cells was actually slightly lower, and probably not different from 1, except for NEM-treated cells where the ratio was about 4. These data point to a symmetric inhibition for swollen and A23187-treated cells, whereas for NEM activation a real asymmetry appears to exist. This finding will be interpreted in the Discussion.

Because K efflux was determined in the absence of Rb_o, whereas Rb influx was measured in the presence of 20 mM Rb_o, this could explain the asymmetry observed. Thus, we performed control experiments to measure K efflux in the presence and absence of Rb_o and determined the percentage of inhibition, IC_{50}s and the drug-sensitive

Table 3. Quinine (Q)- or Quinidine (QD)-sensitive, Cl-dependent K and Rb fluxes at 1 mM drug concentration

Treatment	Efflux*		Influx*	Efflux/influx ratio
	Q	QD	QD	QD
Swelling	0.50 ± 0.08 (7)	0.58 ± 0.19 (3)	0.74 (2)	0.78
NEM	1.53 ± 0.17 (3)	2.9 (2)	0.71 ± 0.28 (5)	4.08
A23187	0.97 (2)	0.97 (2)	1.37 ± 0.55 (3)	0.71

* Results are expressed in mmol/LOC × hr.

Cl-dependent flux for Q and QD, as described in Table 3. The results obtained indicated that lack of Rb_o in K efflux measurements was not the cause of the asymmetry observed (*results not shown*).

Discussion

This study shows for the first time inhibition of Cl-dependent K and Rb fluxes by antimalarial drugs. Previous reports in human red cells by Garay et al. [14] and Kaji [21], and in LK SRBCs by Ellory and Dunham [13] indicated no inhibition of this transporter by Q. Since the membrane lipid composition of human and sheep RBCs is different, it is possible that higher IC_{50}s are required to inhibit this transporter in human red cells and that the concentrations of 0.1 mM for the NEM-K efflux [14] and 0.5 mM for swelling-activated K influx [21] were not sufficient to produce inhibition. Likewise, in LK SRBCs the Q concentration required to block K influx may be higher than the one tested in the study by Ellory and Dunham [13]. In our study we chose not to test the inhibition of Rb influx by Q due to the higher lysis induced by this drug.

Mechanism of Q and QD Inhibition

Due to their amphipilic nature, these cationic quaternary amines are expected to partition in the membrane and interact nonspecifically with the membrane lipids and thus affect indirectly the function of membrane proteins by inducing disruption of the lipid bilayer [9] and, depending on the conditions, lipid peroxidation as well [36]. The increased cell lysis with time and concentration shown in Fig. 3 may support such mechanisms. In addition to these effects, membrane-active drugs, such as Q and QD, can interact specifically or unspecifically with membrane proteins [9]. The data in Fig. 3 may support nonspecific interactions of Q and QD with membrane proteins. Another mechanism of Q and QD inhibition could be by inducing cell shrinkage which inhibits the K-Cl cotransport [26]. These amphiphilic amines are known to change the pH_i, a reason why we determined water and Cl contents. However, we found that in contrast to a reduction in cell volume and hence secondary inhibition of Cl-dependent K and Rb fluxes, the cells actually swelled and gained Cl upon treatment with Q and did not change volume but lost Cl with QD. These results are inconsistent with a change in pH which should be the same for the two drugs since they are stereoisomers. Furthermore, the changes in volume and Cl cannot be explained in connection with the inhibitory effect of the drugs on K(Rb)-Cl fluxes since they correspond to total water and Cl contents.

In light of the numerous studies in which especially Q is used as a channel blocker, our findings raise questions about the nature, i.e., carrier *vs.* channel, of the K-Cl "cotransport" and the possibility that we are dealing with coupled K and Cl channels, as they occur during RVD in HeLa cells incubated in Na-free high K medium [20]. Although studies by Brugnara et al. [4] and Kaji [22] have clearly demonstrated that K-Cl cotransport is electroneutral and independent of membrane potential, factors such as symmetry of inhibition need to be considered to reassess this point. A symmetric inhibition, in absolute flux units of mass/(area × time), is to be expected for an obligatory exchange system whereas asymmetric inhibition is frequently observed in channels (Table 1, Chapter 15, Ref. [18]). Tables 1 and 2 show, in general, asymmetric inhibition of K(Rb)-Cl fluxes and support the notion that these fluxes behave as if channel mediated. However, the percentage of inhibition as a fraction of the maximum inhibitable component [$K(Rb)ClP_{1(H)}$] originated IC_{50}s and efflux/influx ratios (Table 2) expected for a carrier mechanism. Results in Table 3 also appear to support coupled Cl-dependent K and Rb fluxes in cells activated by swelling and A23187 but not by NEM.

Effect of QD on NEM-activated Cells and in NO_3 Medium

The higher efflux/influx ratio observed in NEM-treated cells (*see* Table 3) could result from activation by NEM of a Cl-dependent QD-sensitive K efflux different from that observed in the other two types of cells. This idea is supported by the fact that the influx components are similar in magnitude for the three manipulations (*see* Table 3). This finding is preliminary at this point and needs further investigation.

QD inhibited K and Rb fluxes in NO_3, whereas the effect of Q was more variable. It is possible that QD was inhibiting an additional component which may be present both in Cl and NO_3. While at this point we do not have an explanation for the effect of QD in NO_3, in our analysis of K(Rb)-Cl fluxes this effect was excluded.

In summary, heterogeneity of Cl-dependent K(Rb)

fluxes, uncovered by Q and QD, appears to explain the observed asymmetries in SRBCs.

Cinchona Bark Derivatives and Sickle Cell Anemia

Based on this and studies by others, cinchona bark derivatives should be expected to exert their effect on malaria infection via multiple mechanisms of action due to the diversity of functions described above. In this study we show that antimalarial drugs do inhibit K-Cl cotransport. However, to inhibit the Ca-activated K channel and the K(Rb)Cl flux, both mechanisms thought to play an important role in cell dehydration, drugs with higher potency than Q and QD may find application in the treatment of sickle cell anemia.

We thank Dr. Luo Lu from the Department of Physiology and Biophysics for helpful discussions, Mrs. Samyuktha Ramalingam for excellent technical assistance, undergraduate summer student, Salman Elmi, for assisting in the calculations, and the Word Processing Center of Wright State University School of Medicine for typing of this manuscript.

This work was supported by a grant from the National Institutes of Health (NIH DK5RO1 37,160).

References

1. Adragna, N.C., Lauf, P.K. 1994. Quinine and quinidine inhibit K-Cl cotransport in low K sheep erythrocytes. *Biophys. J.* **66:**A32 (*Abstr.*)
2. Ahmad, S., Phillips, R.S., Stammer, C.H. 1992. Inhibition of pig kidney L-aromatic aminoacid decarboxylase by 2,3-methano-m-tyrosines. *J. Med. Chem.* **35:**1410–1417
3. Bookchin, R.M., Ortiz, O.E., Lew, V.L. 1991. Evidence for a direct reticulocyte origin of dense red cells in sickle cell anemia. *J. Clin. Invest.* **87:**113–124
4. Brugnara, C., Van Ha, T., Tosteson, D.C. 1989. Role of chloride in potassium transport through a K-Cl cotransport system in human red cells. *Am. J. Physiol.* **256:**C994–C1003
5. Covinsky, J.O., Conn, R.D. 1981. Quinidine. Therapeutic use and serum concentration monitoring. In: Individualizing Drug Therapy. Practical Applications of Drug Monitoring. W.J. Taylor and A.L. Finn, editors. pp. 111–132. Gross, Townsend, Frank, New York
6. Cowan, C.L., Cohen, R.A. 1992. Different mechanisms of relaxation of pig coronary artery to bradykinin and cromakalim are distinguished by potassium channel blockers. *J. Pharmacol. Exp. Ther.* **260:**248–253
7. Cummings, T.A., Kinnamon, S.C. 1992. Apical K^+ channels in *Necturus* taste cells. Modulation by intracellular factors and taste stimuli. *J. Gen. Physiol.* **99:**591–613
8. Dahl, M.L., Nordin, C., Bertilsson, L. 1991. Enantioselective hydroxylation of nortriptyline in human liver microsomes, intestinal homogenate, and patients treated with nortriptyline. *Ther. Drug Monit.* **13:**189–194
9. Deuticke, B., Grebe, R., Haest, C.W.M. 1990. Action of drugs on the erythrocyte membrane. *Blood Cell. Bioch.* **1:**475–529
10. Discala, F., Belachgar, F., Planelles, G., Hulin, P., Anagnostopoulos, T. 1992. Barium- or quinine-induced depolarization activates K^+, Na^+ and cationic conductances in frog proximal tubular cells. *J. Physiol.* **448:**525–537
11. Dunham, P.B. 1990. K,Cl cotransport in mammalian erythrocytes. *In:* Regulation of Potassium Transport across Biological Membranes. L. Reuss, J.M. Russel, and G. Szabo, editors. pp. 331–360. University of Texas Austin
12. el Benna, J., Pasquier, C., Labro, M.T. 1991. Quinine uptake by human polymorphonuclear neutrophils. *Antimicrob. Agents Chemother.* **35:**1474–1478
13. Ellory, J.C., Dunham, P.B. 1980. Volume-dependent passive potassium transport in LK sheep red cells. *In:* Membrane Transport in Erythrocytes. Alfred Benzon Symposium 14. U. Lassen, H.H. Ussing, and J.O. Wieth, editors. pp. 409–425. Munskgaard, Copenhagen
14. Garay, R.P., Nazaret, C., Hannaert, P.S., and Cragoe, E.J., Jr. 1988. Demonstration of a [K^+,Cl]-cotransport system in human red cells by its sensitivity to [(Dihydroindenyl)oxy]alkanoic acids: regulation of cell swelling and distinction from the bumetanide-sensitive [Na^+,K^+,Cl^-]-cotransport system. *Mol. Pharmacol.* **33:**696–701
15. Gendrel, D., Kombila, M., Nardou, M., Gendrel, C., Djouba, F., Martz, M., Richard-Lenoble, D. 1992. Malaria and Hemoglobin S: Interactions in African children. *Presse Med.* **21:**887–890
16. Goldstein, J.L., Fogelson, B.G., Snow, J.C., Schmidt, L.N., Mozwecz, H., Layden, T.J. 1993. Rabbit esophageal cells possess K^+ channels: effect of hyposmotic stress on channel activity. *Gastroenterology* **104:**417–426
17. Halsberg, A., Romanin, C., Koerber, R. 1992. Membrane potential modulates release of tumor necrosis factor in lipopolysaccharide-stimulated mouse macrophages. *Mol. Biol. Cell* **3:**451–460
18. Hille, B. 1992. Ionic Channels of Excitable Membranes. pp. 291–314, 390–422. Sinauer Associates, Sunderland, MA
19. Hughes, I.E., Ilett, K.F., Jellett L.B. 1975. The distribution of quinidine in human blood. *Br. J. Clin. Pharmacol.* **2:**521–525
20. Ikehara, T., Takahashi, A., Yamaguchi, H., Hosokawa, K., Masuya, T., Miyamoto, H. 1991. Regulatory changes in the K^+, Cl^- and water contents of HeLa cells incubated in an isosmotic high $K(^+)$-medium. *Biochim. Biophys. Acta* **1068:**87–96
21. Kaji, D. 1986. Volume-sensitive K transport in human erythrocytes. *J. Gen. Physiol.* **88:**719–738
22. Kaji, D. 1992. Effect of varying membrane potential on K-Cl cotransport in human erythrocytes. *Am. J. Physiol.* **264:**C376–C382
23. Karbwang, J., Molunto, P., Bunnag, D., Harinasuta, T. 1991. Plasma quinine levels in patients with falciparum malaria when given alone or in combination with tetracycline with or without primaquine. *Southeast Asian J. Trop. Med. Public Health* **22:**72–76
24. Lauf, P.K. 1983. Thiol-dependent passive K/Cl transport in sheep red cells. I. Dependence on chloride and external $K^+(Rb^+)$ions. *J. Membrane Biol.* **73:**237–246
25. Lauf, P.K., 1988. Volume and anion dependency of ouabain-resistant K-Rb fluxes in sheep red blood cells. *Am. J. Physiol.* **255:**C331–C339
26. Lauf, P.K., Bauer, J., Adragna, N.C., Fujise, H., Zade-Oppen, A.M., Ryu, K.H., Delpire, E. 1992. Erythrocyte K-Cl cotransport: properties and regulation. *Am. J. Physiol.* **263:**C917–C932
27. Lauf, P.K., Erdmann, A., Adragna, N.C. 1994. Response of K-Cl cotransport to pH and cellular magnesium in volume-clamped low K sheep erythrocytes: three equilibrium states. *Am. J. Physiol.* **266:** C95–C103
28. Luchi, R., Helwig, J., Jr., Conn, H., Jr. 1963. Quinidine toxicity and its therapy: An experimental study. *Am. Heart J.* **65:**340–348
29. Murakami, M., Takada, K., Muranishi, S. 1992. Further mechanistic study on intestinal absorption enhanced by unsaturated fatty

acids: Reversible effect by sulfhydryl modification. *Biochem. Biophys. Acta* **117:**83–89

30. Muralidharan, G., Hawes, E.M., McKay, G., Korchinski, E.D., Midha, K.K. 1991. Quinidine but not quinine inhibits in man the oxidative metabolic routes of methoxyphenamine which involve debrisoquine 4-hydroxylase. *Eur. J. Clin. Pharmacol.* **41:**471–474
31. Muralidharan, G., Hawes, E.M., McKay, G., Midha, K.K. 1991. Quinine is a more potent inhibitor than quinidine in rat of the oxidative metabolic routes of methoxyphenamine which involve debrisoquine 4-hydroxylase. *Xenobiotica* **21:**1441–1450
32. Ott, R.J., Hui, A.C., Wong, F.M., Hsyu, P.H., Giacomini, K.M. 1991. Interactions of quinidine and quinine and (+)- and (−)-pindolol with the organic cation/proton antiporter in renal brush-border membrane vesicles. *Biochem. Pharmacol.* **41:**142–145
33. Sabchareon, A., Chongsuphajaisiddhi, T., Attanath, P., Singhasivanon, V., Acmor-Apolinar, M.M., Pojjaroen-Anant, C. 1991. Red cell plasma concentrations of combined quinine-quinidine and quinine in falciparum malaria. *Ann. Trop. Paediatr.* **11:**315–324
34. Schlatter, E., Bleich, M., Hirsch, J., Markstahler, U., Frobe, U., Greger, R. 1993. Cation specificity and pharmacological properties of the $Ca^{(2+)}$-dependent K^+ channel of rat cortical collecting ducts. *Pfluegers Arch.* **422:**481–491
35. Slater, A.F.G., Ceramil, A. 1992. Inhibition by chloroquine of a novel haem polymerase enzyme activity in malaria trophozoites. *Nature* **355:**167–169
36. Sugioka, Y., Suzuki, M. 1991. The chemical basis for the ferriprotoporphyrin IX-chloroquine complex induced lipid peroxidation. *Biochim. Biophys. Acta* **1074:**19–24
37. Takeuchi, S., Marcus, D.C., Wangemann, P. 1992. Maxi K^+ channel in apical membrane of vestibular dark cells. *Am. J. Physiol.* **262:**C1430–1436
38. Wang, H., Grahame-Smith, D.G. 1992. The effects of rubidium, caesium and quinine on 5-HT-mediated behaviour in rat and mouse. *3. Quinine. Neuropharmacology* **31:**425–431
39. Warrell, D.A. 1992. Cerebral Malaria. *Schweiz Med. Wochenschr.* **122:**879–886
40. Watt, G., Shanks, G.D., Edstein, M.D., Pavanand, K., Webster, H.K., Wechgritaya, S. 1991. Ciprofloxacin treatment of drug-resistant falciparum malaria. *J. Infect. Dis.* **164:**602–604
41. Xiao, J., Nie, L.H., Yao, S.Z. 1991. Transfer mechanism of quinine drug across the oil/water (O/W) interface. *Sci. China B* **34:**42–53